60B Solid solutions

No. 60B-1 $(NH_2CH_2COOH)_3 \cdot H_2SO_4$–$(NH_2CH_2COOH)_3 \cdot H_2SeO_4$ (TGS–TGSe)

1b	Phase diagram: Fig. 60B-1-001; see also Fig. 60B-2-001 in No. 60B-2. Properties of L-alanine doped crystals: Table 60B-1-001.	
2a	Composition of solid solution as a function of composition of growing solution: Fig. 60B-1-002; see also	71Bre
5a	Dielectric constant: Table 60B-1-002; Fig. 60B-1-003; see also For L-alanine doped crystals: see Table 60B-1-001. Effect of hydrostatic pressure on Curie-Weiss constant: Fig. 60B-1-004. $d\Theta_f/dp$: Fig. 60B-1-005.	82Pol
b	Non-linear dielectric properties: see	59Fat
d	Pyroelectric coefficient: Table 60B-1-001, Table 60B-1-002; Fig. 60B-1-003.	
6a	Effect of hydrostatic pressure on heat capacity: Fig. 60B-1-006. Heat capacity of L-alanine doped crystals: Table 60B-1-001.	
9a	Refractive index: Fig. 60B-1-007, Fig. 60B-1-008.	
11	Electrical resistivity: see Table 60B-1-002. For L-alanine doped crystals: see Table 60B-1-001.	
16	Effect of X-ray irradiation: see Table 60B-1-002.	

Table 60B-1-001. $[(NH_2CH_2COOH)_3 \cdot H_2SO_4]_x[(NH_2CH_2COOH)_3 \cdot H_2SeO_4]_{1-x}$ (TGS–TGSe) with L-alanine addition. Properties at 21 °C [76Bye].

% L-alanine in solution	x in solution	x in crystal	Θ_f [°C]	$\rho_{d.c.}$ [Ωm]	$\rho_{1.6\,kHz}$ [Ωm]	$\kappa_{1.6\,kHz}$	p_2 [10^{-4} C K^{-1} m^{-2}]	ρc_p [10^6 J m^{-3} K^{-1}]	ρ [10^3 kg m^{-3}]
40	1	1	49.5	$2 \cdot 10^{13}$	$1.4 \cdot 10^8$	27	3.6	2.1	1.69
20	0.75	0.92	46.8	$3 \cdot 10^{11}$	$3.1 \cdot 10^8$	34	4.0	2.2	–
20	0.60	0.89	45.6	$5 \cdot 10^{12}$	$3.3 \cdot 10^7$	36	3.8	2.0	–
20	0.35	0.70	40.6	$3 \cdot 10^{12}$	$2.1 \cdot 10^8$	41	6.1	2.0	–
20	0.15	0.38	32.1	$3 \cdot 10^{10}$	$1.4 \cdot 10^7$	65	7.1	2.0	–
20	0.05	0.16	26.3	$3 \cdot 10^{11}$	$5.6 \cdot 10^7$	122	12.2	1.9	–
40	0	0	22.5	$2.5 \cdot 10^{12}$	$7.0 \cdot 10^6$	364	28.7	1.8	1.87

Table 60B-1-002. $[(NH_2CH_2COOH)_3 \cdot H_2SO_4]_x[(NH_2CH_2COOH)_3 \cdot H_2SeO_4]_{1-x}$ (TGS–TGSe). Pyroelectric coefficient, dielectric constant and electrical resistivity at 21 °C before and after X-ray irradiation/field treatment for 1 h [76Bye].

x	p_2 [10^{-4} C K^{-1} m^{-2}]		$\kappa_{1.6\,kHz}$		ρ [10^7 Ωm]	
	Before	After	Before	After	Before	After
1.00	3.5	4.0	38	30	1.2	10
0.95	3.4	4.1	26	26	1.5	4.5
0.90	3.5	4.0	40	30	1.5	2.2
0.80	3.0	4.9	38	38	1.3	2.1
0.35	5.6	9.8	73	120	0.6	0.3
0.05	14.8	17.5	220	130	0.2	0.3
0	42	10	420	1000	0.01	0.4

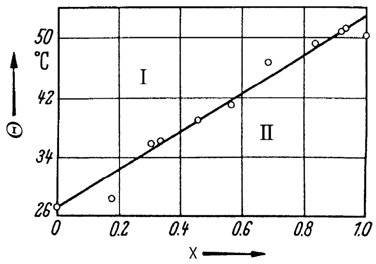

Fig. 60B-1-001. $[(NH_2CH_2COOH)_3 \cdot H_2SO_4]_x[(NH_2CH_2COOH)_3 \cdot H_2SeO_4]_{1-x}$ (TGS–TGSe). Phase diagram [59Fat].

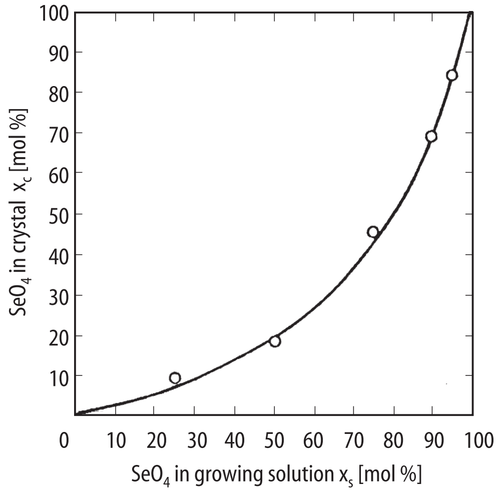

Fig. 60B-1-002. $[(NH_2CH_2COOH)_3 \cdot H_2SO_4]_x[(NH_2CH_2COOH)_3 \cdot H_2SeO_4]_{1-x}$ (TGS–TGSe). x_c vs. x_s [59Fat]. x_c: mol% of SeO_4 in crystal. x_s: mol% of SeO_4 in growing solution.

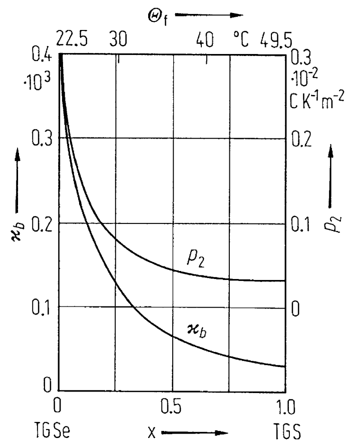

Fig. 60B-1-003. $[(NH_2CH_2COOH)_3 \cdot H_2SO_4]_x[(NH_2CH_2COOH)_3 \cdot H_2SeO_4]_{1-x}$ (TGS–TGSe). κ_b, p_2 vs. x [76Bye]. $T = 21$ °C. $f = 1.6$ kHz. Θ_f of the composition is given at the top as an alternative abscissa.

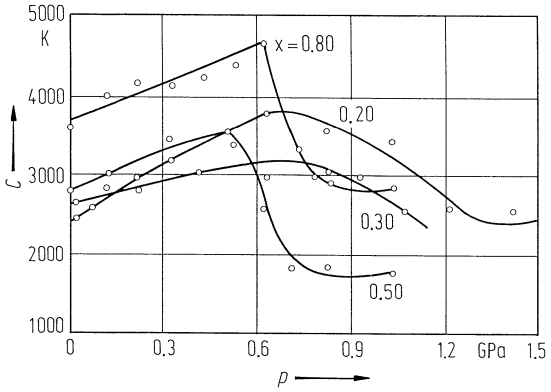

Fig. 60B-1-004. $[(NH_2CH_2COOH)_3 \cdot H_2SO_4]_x[(NH_2CH_2COOH)_3 \cdot H_2SeO_4]_{1-x}$ (TGS–TGSe). C vs. p [82Pol]. Parameter: x. C: Curie-Weiss constant.

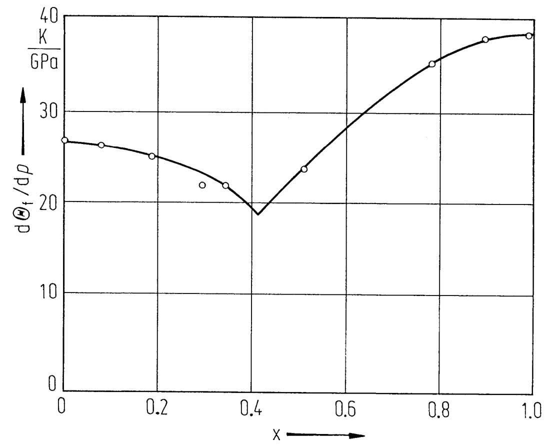

Fig. 60B-1-005. $[(NH_2CH_2COOH)_3 \cdot H_2SO_4]_x[(NH_2CH_2COOH)_3 \cdot H_2SeO_4]_{1-x}$ (TGS–TGSe). $d\Theta_f/dp$ vs. x [82Pol]. p: hydrostatic pressure.

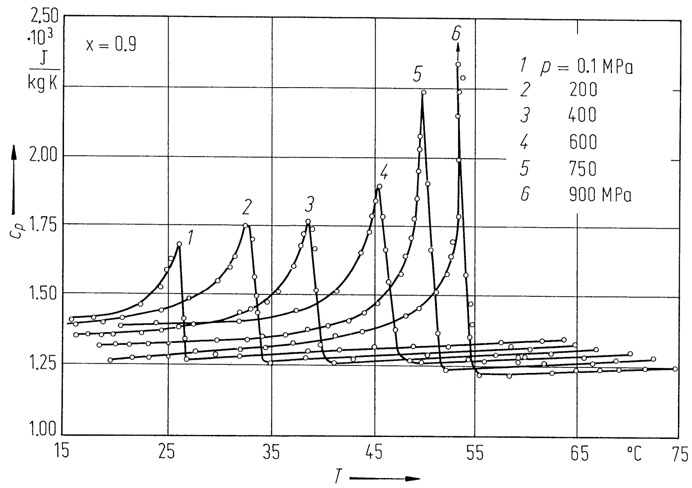

Fig. 60B-1-006. $[(NH_2CH_2COOH)_3 \cdot H_2SO_4]_x[(NH_2CH_2COOH)_3 \cdot H_2SeO_4]_{1-x}$ (TGS–TGSe, x = 0.9). c_p vs. T [83Gul]. c_p: specific heat capacity at constant pressure. Parameter: p.

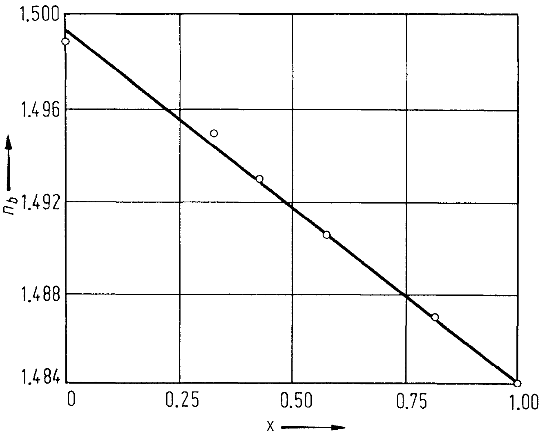

Fig. 60B-1-007. $[(NH_2CH_2COOH)_3 \cdot H_2SO_4]_x[(NH_2CH_2COOH)_3 \cdot H_2SeO_4]_{1-x}$ (TGS–TGSe). n_b vs. x [72Hon].

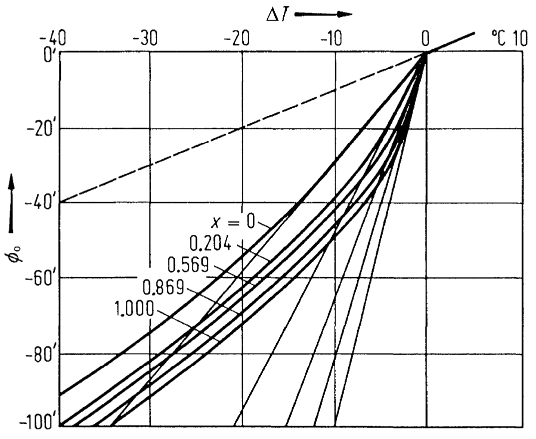

Fig. 60B-1-008. $[(NH_2CH_2COOH)_3 \cdot H_2SO_4]_x[(NH_2CH_2COOH)_3 \cdot H_2SeO_4]_{1-x}$ (TGS–TGSe). ϕ_o vs. ΔT [68Bre]. Parameter: x. ϕ_o: rotation angle of the optical indicatrix around the *b* axis. $\Delta T = T - \Theta_f$.

References

59Fat Fatuzzo, E., Nitsche, R.: Z. Elektrochem. **63** (1959) 970.

68Bre Brezina, B., Galanov, E.K., Ivanov, N.R., Kislovskii, L.D., Shuvalov, L.A.: Kristallografiya **13** (1968) 821; Sov. Phys. Crystallogr. (English Transl.) **13** (1969) 710.

71Bre Brezina, B.: Mater. Res. Bull. **6** (1971) 401.

72Hon Honeyman, W.N., Lee, M.K.: J. Phys. D **5** (1972) 188.

76Bye Bye, K.L., Whipps, P.W., Keve, E.T., Josey, M.R.: Ferroelectrics **11** (1976) 525.

82Pol Polandov, I.N., Varikash, V.M., Gulish, O.K.: Vestn. Mosk. Univ. Khim. **37** (1982) 401; Moscow Univ. Chem. Bull. (English Transl.) **37** (1982) 109.

83Gul Gulish, O.K., Polandov, I.N., Kuyumchev, A.A.: Fiz. Tverd. Tela **25** (1983) 2115; Sov. Phys. Solid State (English Transl.) **25** (1983) 1217.

No. 60B-2 $(NH_2CH_2COOH)_3 \cdot H_2SO_4$–$(NH_2CH_2COOH)_3 \cdot H_2BeF_4$ (TGS–TGFB)

1b	Transition temperature: Table 60B-2-001; Fig. 60B-2-001.	
2a	Composition of solid solution as a function of composition of growing solution: Fig. 60B-2-002.	
3a	Unit cell parameters: Table 60B-2-001; see also	92Zhe
5a	Dielectric constant: Fig. 60B-2-003.	
c	Spontaneous polarization: Fig. 60B-2-004.	
d	Pyroelectric coefficient: Fig. 60B-2-005.	
10a	Raman scattering: see	90YiJ

Table 60B-2-001. $[(NH_2CH_2COOH)_3 \cdot H_2SO_4]_{1-x}[(NH_2CH_2COOH)_3 \cdot H_2BeF_4]_x$ (TGS–TGFB). Unit cell parameters at room temperature and transition temperature [90YiJ]. Crystallographic axial system by Hoshino et al. is adopted, see subsection 3a in No. 60A-1.

	x = 0.0	x = 0.2	x = 0.4	x = 1.0
a' [Å]	9.436	9.413	9.410	9.402
b' [Å]	12.686	12.645	12.650	12.603
c' [Å]	5.742	5.736	5.731	5.739
β' [°]	110.27	110.21	110.17	110.26
V [Å^3]	644.7	640.7	640.3	637.9
Θ_f [°C]	49	55	60	74

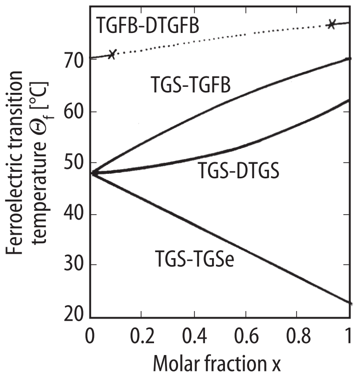

Fig. 60B-2-001. $[(NH_2CH_2COOH)_3 \cdot H_2SO_4]_{1-x}[(NH_2CH_2COOH)_3 \cdot H_2BeF_4]_x$ (TGS–TGFB), $[(NH_2CH_2COOH)_3 \cdot H_2SO_4]_{1-x}[(NH_2CH_2COOH)_3 \cdot H_2SeO_4]_x$ (TGS–TGSe), $[(NH_2CH_2COOH)_3 \cdot H_2SO_4]_{1-x}[(ND_2CH_2COOD)_3 \cdot D_2SO_4]_x$ (TGS–DTGS), $[(NH_2CH_2COOH)_3 \cdot H_2BeF_4]_{1-x}[(ND_2CH_2COOD)_3 \cdot D_2BeF_4]_x$ (TGFB–DTGFB). Θ_f vs. x [71Bre].

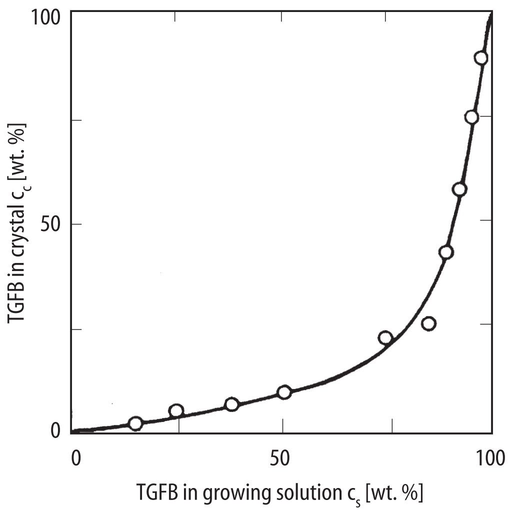

Fig. 60B-2-002. $[(NH_2CH_2COOH)_3 \cdot H_2SO_4]_{1-x}[(NH_2CH_2COOH)_3 \cdot H_2BeF_4]_x$ (TGS–TGFB). c_c vs. c_s [71Bre]. c_c: concentration of TGFB in crystal. c_s: concentration of TGFB in growing solution.

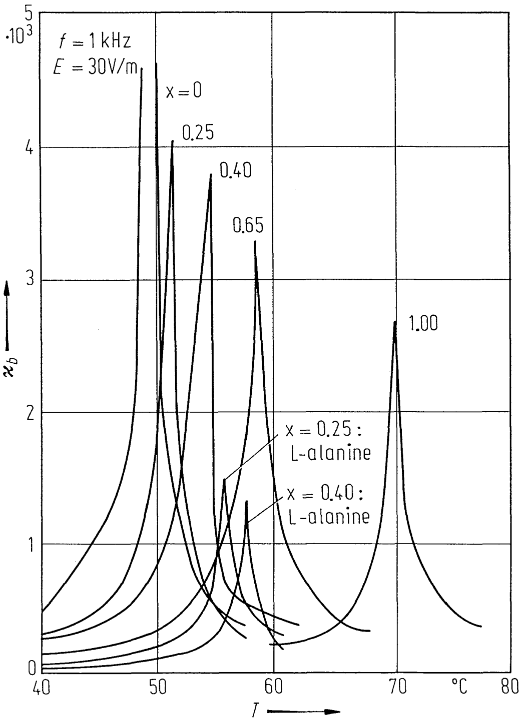

Fig. 60B-2-003. $[(NH_2CH_2COOH)_3 \cdot H_2SO_4]_{1-x}[(NH_2CH_2COOH)_3 \cdot H_2BeF_4]_x$ (TGS–TGFB). κ_b vs. T [81Mat]. Parameter: x. Two specimens contain 0.25 % L-alanine.

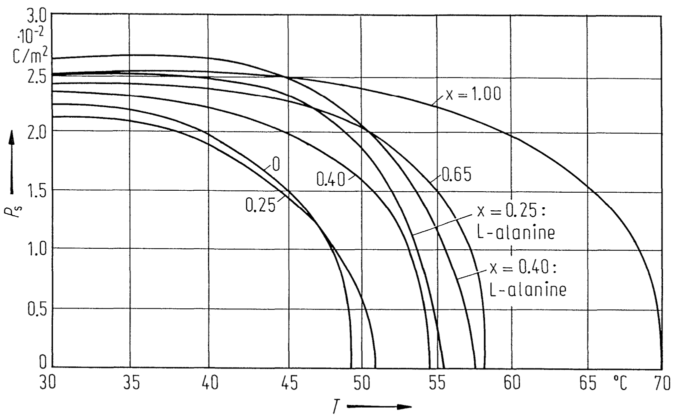

Fig. 60B-2-004. $[(NH_2CH_2COOH)_3 \cdot H_2SO_4]_{1-x}[(NH_2CH_2COOH)_3 \cdot H_2BeF_4]_x$ (TGS–TGFB). P_s vs. T [81Mat]. Parameter: x. Two specimens contain 0.25 % L-alanine.

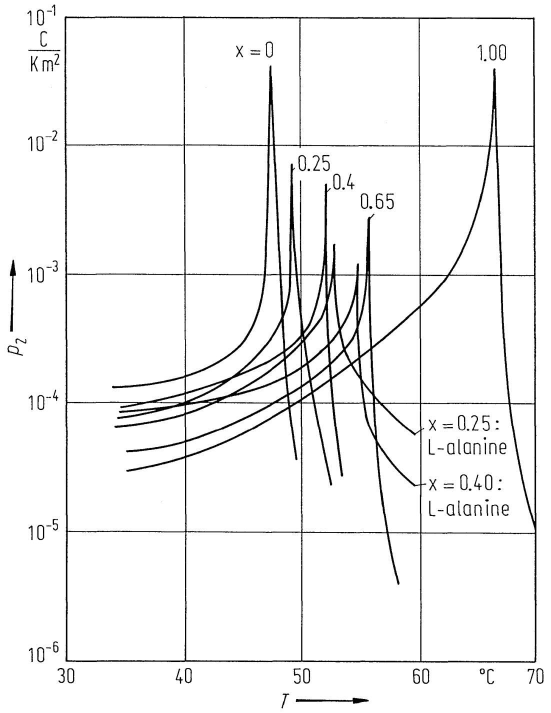

Fig. 60B-2-005. $[(NH_2CH_2COOH)_3 \cdot H_2SO_4]_{1-x}[(NH_2CH_2COOH)_3 \cdot H_2BeF_4]_x$ (TGS–TGFB). p_2 vs. *T*. [81Mat]. Parameter: x. Two specimens contain 0.25 % L-alanine. p_2: pyroelectric coefficient along the *b* axis.

References

71Bre Brezina, B.: Mater. Res. Bull. **6** (1971) 401.
81Mat Mathur, S.C., Batra, A.K., Singh, H., Mansingh, A.: Ferroelectrics **39** (1981) 1197.
90YiJ Yi, J., Lan, G., Li, B., Hu, S., Wang, H., Zhe, J.: Ferroelectrics **101** (1990) 251.
92Zhe Zhe, J., Che, Y.: Chinese Sci. Bull. **37** (1992) 122.

No. 60B-3 $(NH_2CH_2COOH)_3 \cdot H_2SeO_4$–$(NH_2CH_2COOH)_3 \cdot H_2BeF_4$ (TGSe–TGFB)

5a Dielectric constant: Fig. 60B-3-001.
c Spontaneous polarization: Fig. 60B-3-002.

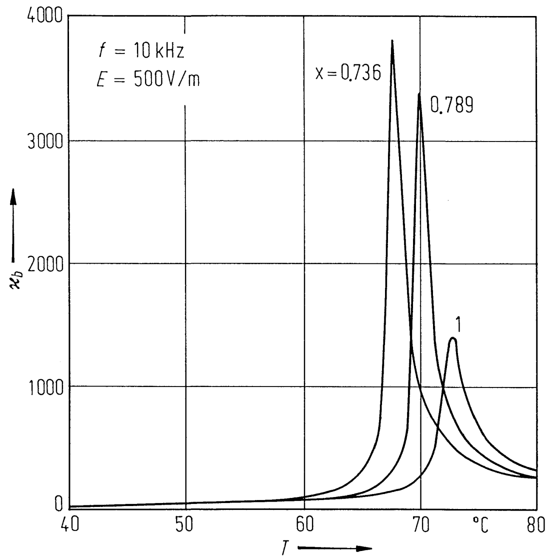

Fig. 60B-3-001. $[(NH_2CH_2COOH)_3 \cdot H_2SeO_4]_{1-x}[(ND_2CH_2COOD)_3 \cdot D_2BeF_4]_x$ (TGSe–DTGFB). κ_b vs. T [82Loi]. Parameter: x.

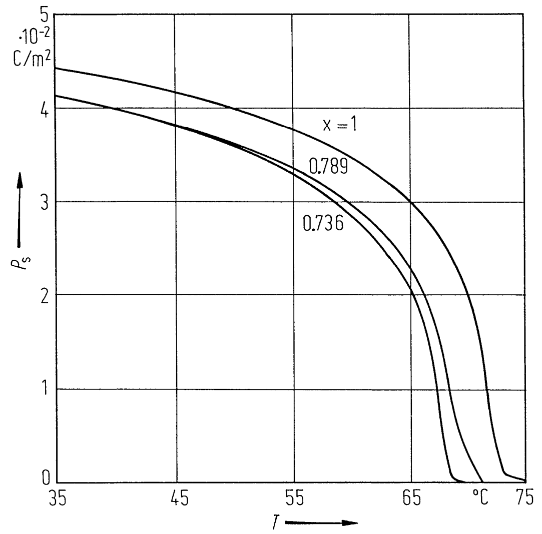

Fig. 60B-3-002. $[(NH_2CH_2COOH)_3 \cdot H_2SeO_4]_{1-x}[(ND_2CH_2COOD)_3 \cdot D_2BeF_4]_x$ (TGSe–DTGFB). P_s vs. T [82Loi]. Parameter: x.

Reference

82Loi Loiacono, G.M., Shaulov, A., Dorman, D., Jacco, J., Kostecky, G.: J. Cryst. Growth **60** (1982) 29.